Radiation Belt Modeling for Spacecraft Design: Model Comparisons for Common Orbits

Jean-Marie Lauenstein, *Member, IEEE*, and Janet L. Barth, *Senior Member, IEEE*

Abstract—We present the current status of radiation belt modeling, providing model details and comparisons with AP-8 and AE-8 for commonly used orbits. Improved modeling of the particle environment enables smarter space system design.

Index Terms—Modeling, radiation belts, trapped particles.

I. INTRODUCTION

ACCURATE space radiation models are important for reducing risk to astronauts and for designing cost-effective, high-performance space systems. The primary models of Earth's radiation belts that are in widespread use are AP-8 [1] and AE-8 [2], released in 1976 and 1983, respectively. The AP-8 models are of trapped protons and include AP-8 MAX and AP-8 MIN, valid for periods of solar maximum and solar minimum, respectively. The AE-8 models for trapped electrons similarly include AE-8 MAX and AE-8 MIN. These standard models are esteemed for their extensive spatial coverage and user friendliness but suffer limitations and inaccuracies [3]-[11]. As contemporary applications demand precision, functionality, and energy coverage not provided by AP-8 and AE-8, new standard radiation belt environment models are needed. In this paper, we assess the current status of radiation belt environment modeling and show comparisons between models. Several compendiums of the Earth's trapped radiation belt models precede this review (e.g. [12]-[15]). This review is motivated by the NASA/Living With A Star (LWS) sponsored international meeting on New Standard Radiation Belt and Space Plasma Models for Spacecraft Engineering, held in Adelphi, Maryland in October 2004. As a result of this international meeting of modelers and space system developers, roadmaps for the development of new standard models are under construction and two interim models are deemed ready for standardization. In light of the progress made towards the replacement of AP-8 and AE-8, this paper provides summaries of the features of the two proposed standard models as well as four other models developed since

the release of AP-8 and AE-8. Importantly, we offer comparisons of these models to AP-8 and AE-8 for four different representative orbits. This information will assist model users in understanding the tools presently available and how they differ from the old standards.

II. TRAPPED RADIATION MODELS

A. The Standard Radiation Belt Models, AP-8 and AE-8

In order to appreciate the need for new models and to assess their potential, the strengths and limitations of the current standard models, AP-8 and AE-8, must be understood. Perhaps the biggest factor driving the continued use of these models lies in the number of years that they have been used to successfully design spacecraft. Their spatial coverage is unmatched by recent modeling efforts: AP-8 is valid from $L = 1.15$ to 6.6; AE-8 covers $L = 1.2$ to 11. The data used to develop them come from 38 satellites [16]; thus, radiation measurements have some degree of inter-instrument validation. This strength is also a source of error in the models due to the challenge of inter-calibrating the instruments. Many of the detector systems whose data were used for these models were never properly calibrated and/or did not have well-defined energy sensitivities [3].

AP-8 and AE-8 are more than 20 years old. The data used to build these models were collected between 1958 and 1979. Due to the dynamic nature of the space environment, the models may no longer portray the environment that today's space systems encounter. Importantly, the inner zone electron flux data are known to be contaminated from high-altitude nuclear-device detonations during the late 1950's and early 1960's [4].

The models must be run with the same internal geomagnetic field models used to analyze the data [5]; as a result, secular changes in the magnetic field that affect the location of the South Atlantic Anomaly (SAA) are not accounted for, resulting in incorrect positions for flux values at low altitudes. Additional low-altitude error results from the absence of east-west asymmetry in the models; while this effect averages out in non-oriented spacecraft, it is important for missions with fixed orientations such as the International Space Station. Dyer presents MIR data highlighting this anisotropy in [6]. At low altitudes, the particle flux gradient becomes very steep due to interactions with the upper atmosphere. Daly and Evans [7] report problems with the interpolation method used in AP-8

J.-M. Lauenstein is with Muñiz Engineering Inc., Lanham, MD 20706 USA (e-mail: Jean.Marie.Lauenstein@gsfc.nasa.gov).

J. L. Barth is with the NASA Goddard Space Flight Center, Greenbelt, MD 20771 USA (e-mail: Janet.L.Barth@nasa.gov).

for this region and provide an improved method of interpolation over the gradient.

Limitations of the AP-8 and AE-8 models also stem from their energy range and temporal resolution. The models do not include fluxes at plasma energies, and stop far short of covering the up to 30 MeV electrons recorded by the CRRES satellite [8]. AP-8 has an energy range of 100 keV to 400 MeV protons, and AE-8 covers 40 keV to 4.5 MeV inner zone electrons and 40 keV to 7 MeV outer zone electrons. The models are static, providing only long-term averages for solar maximum or solar minimum. This division of the cycle into two models does not necessarily parlay into a separation of maximum and minimum flux: there is evidence that the long-term fluctuation of the trapped proton environment is out of phase with the solar cycle [6]. In addition, long-term averaging removes the effects of storm injections and solar wind on flux distributions, preventing use of the models for worst-case analysis and for missions of short duration (<6 months). A clear example of this shortcoming can be found in [9], in which Mazur compares AE-8 with GOES 7 data.

The space systems of today are built using higher-performance technologies that can be more sensitive to radiation. Smaller margins of error in environment estimates will prevent costly over-design and will aid in the decision to use or forego a particular capability.

B. Currently Available Models

General information about the seven publicly available models that this paper addresses can be found in Table 1. The models are organized in the table according to region of coverage. Proton models developed since AP-8 and evaluated here include PSB97 [17], Low Altitude Trapped Radiation Model (LATRM) [18], Trapped Proton Model (TPM-1) [19], and the Combined Release and Radiation Effects Satellite Proton model (CRRESPRO) [20].

Electron models addressed in this paper that were developed since AE-8 include Combined Release and Radiation Effects Satellite Electron model (CRRESELE) [21], Flux Model for Internal Charging (FLUMIC) [22], and the Particle ONERA[1]-LANL[2] Electron (POLE) model [23].

C. Proposed Standards

While ultimately a single model of the radiation belts is desirable, the development of regional models will be pursued in the near-term. A Low Altitude Proton (LAP) model based on TPM-1 and PSB97 has been proposed for standardization. TPM-1, developed with support from the NASA Space Environment Effects Program, is the result of combining elements of LATRM, a low-altitude model from polar data covering almost two solar cycles, with the Air Force Research Laboratory's CRRESPRO, a medium Earth orbit model based on the 14 months of data from the CRRES satellite. PSB97 was developed using one year of data from the Solar, Anomalous, and Magnetospheric Particle Explorer

(SAMPEX) satellite with support from the European Space Agency (ESA); additional SAMPEX data are available from 1992 to the present [17]. The addition of PSB97 and data to the LAP model will extend the low altitude energy coverage to 500 MeV.

POLE, a model of geostationary electrons, has also been proposed for standardization. The model is a result of the collaboration between LANL, with support from NASA's LWS Targeted Research and Technology (TR&T) Program, and ONERA. POLE is based on datasets from 13 LANL geostationary satellites covering the period 1976-2001. In the future, the energy range of the model will likely be extended beyond the current 2.5 MeV upper limit [23].

The decision to standardize new models will be made by the Committee on Space Research/Panel for Radiation Belt Environment Modeling (COSPAR/PRBEM); inclusion of models in this paper should not be viewed as an endorsement. Details about the PRBEM and standardization process can be found at http://www.cosparhq.org/scistr/prbem.htm and links therein.

III. COMPARISONS WITH AP-8 AND AE-8

A. Proton Models

We have generated average flux spectra from the trapped proton models for three commonly used orbits in order to present meaningful comparisons between the models. Orbits include an International Space Station (ISS)-like low Earth orbit (LEO), a low Earth polar orbit, and an elliptical medium Earth orbit (MEO). Average proton flux was calculated from a sampling of 20 revolutions per right ascensions of ascending node (Ω) of 0°, 90°, 180°, and 270°, during 2007 for solar minimum and 2012 for solar maximum. AP-8, CRRESPRO, and PSB97 average fluxes were generated with the ESA Space Environment Information System (SPENVIS); TPM-1 and LATRM were run using the same ephemeris file from the SPENVIS SAPRE orbit generator. SPENVIS uses the Jensen and Cain 1960 internal field model for AP-8 MIN and the Goddard Space Flight Center (GSFC) 12/66 field model extrapolated to 1970 for AP-8 MAX, as recommended in [5].

1) Low Earth Orbit

Fig. 1 shows the results for an ISS-type circular low Earth orbit of 400 km altitude and 51.6° inclination during solar minimum. Both differential flux (filled symbols) and integral flux (unfilled symbols) are graphed according to model capability. The consensus of the post-AP8 models suggests that AP-8 under-predicts proton flux above 10 MeV by more than a factor of two for this orbit. Actual factor differences from AP-8 can be found in Table 2 for 1.5 MeV, 20 MeV, 60 MeV, and 100 MeV protons. In the table, the integral and differential flux predicted by AP-8 are given, along with the ratio of each post-AP-8 model flux versus the AP-8 predicted flux. When a model is not valid for a given energy value, a line is drawn through the table cell. As can be seen by the factor differences in Table 2 for energies 20 MeV and above, previously reported factor of two corrections [e.g. 10] may be

too low.

For lower energies, TPM-1 predicts as much as a factor of nine (at 1.5 MeV-2 MeV) less average flux than does AP-8 during solar minimum, and a factor of two less during solar maximum (see Fig. 2 and Table 2). The validity of the AP-8 model for energies below 10 MeV is uncertain [10], [24]. Armstrong and Colborn [10] suggest using data from the S3-3 satellite as an alternative to AP-8 for very low energy spectra. It is notable therefore that TPM-1's under-prediction of AP-8 for low energies is in contrast to these S3-3 data which over-predict AP-8 at low altitude [24]. Our findings are in keeping with those of the TPM-1 developer [19].

In Fig. 2, TPM-1 is compared to AP-8 for periods of both solar minimum (grey symbols) and solar maximum (black symbols). For 10 MeV and lower energy protons, TPM-1 suggests a smaller variation of flux with the solar cycle than does AP-8.

2) Low Earth Polar Orbit

Fig. 3 shows the results for a low Earth polar orbit of 800 km altitude and 98° inclination during solar minimum. Both differential flux (filled symbols) and integral flux (unfilled symbols) are graphed according to model capability. Newer models predict a harder proton flux spectrum for this orbit than does AP-8, suggesting a factor of two or more greater flux for energies above 8 MeV. See Table 3 for comparisons at specific energies. As can be seen in Fig. 3, for energies above 100 MeV, PSB97 predicts more than a factor of five greater flux at solar minimum for this orbit.

For lower energies, TPM-1 predicts as much as a factor of nine (at 1.5 MeV) less average flux than does AP-8 during solar minimum, and a factor of seven less during solar maximum, as shown in Fig. 4 and Table 3. For this orbit, both AP-8 and TPM-1 show similar variation between solar maximum and solar minimum proton flux (Fig. 4).

3) Medium Earth Orbit

Average differential proton flux was determined from AP-8, TPM-1, and CRRESPRO for an elliptical orbit of 2000 km perigee, 26,750 km apogee, 63.4° inclination, and 270° argument of perigee. CRRESPRO is valid for solar maximum only; comparisons are therefore made for this part of the solar cycle. Both TPM-1 and CRRESPRO (on which TPM-1 is partly based) contain models for normally quiet geomagnetic periods and for active geomagnetic periods such as the March 1991 event that occurred during the CRRES mission.

For quiet geomagnetic periods of solar maximum (Fig. 5), CRRESPRO predicts about a factor of three lower average proton flux than AP-8. The difference peaks to a factor of nine in the 15-20 MeV range. Conversely, for active periods of solar maximum (Fig. 6), CRRESPRO shows agreement with AP-8, though with a divergence in the 15-20 MeV range of up to a factor of six less flux. Table 4 provides factor differences between the CRRESPRO models and AP-8 at 1.5 MeV, 10 MeV, 20 MeV, and 60 MeV energy levels.

TPM-1 suggests an order of magnitude less flux than AP-8 for quiet periods of solar maximum (Fig. 5). The difference grows to a factor of 40 less flux at 10 MeV. For active

geomagnetic periods, TPM-1 predicts lower flux by more than a factor of four for <10 MeV, and at most a factor of 20 in the 15-20 MeV range (Fig. 6). See Table 4 for factor differences with AP-8 at specific energy levels.

B. Electron Models

Average integral flux spectra for the trapped electron models were generated for two common orbits: an elliptical medium Earth orbit and a geostationary orbit (GEO). The average electron flux was calculated from a sampling of 20 revolutions per right ascensions of ascending node (Ω) of 0°, 90°, 180°, and 270° for MEO. For GEO, 2 revolutions at 82°W longitude were used. An exception is FLUMIC, which as packaged within the internal charging code, DICTAT, generates average flux based on a one-revolution sampling. Mission dates are 2007 for solar minimum and 2012 for solar maximum. AE-8, CRRESELE, and FLUMIC average fluxes were generated with SPENVIS; POLE was run using the same ephemeris file from the SPENVIS SAPRE orbit generator. SPENVIS uses the Jensen and Cain 1960 internal field model for AE-8 MIN and MAX, as recommended in [5].

1) Medium Earth Orbit

Average integral electron flux was determined for an elliptical orbit of 8000 km x 26,750 km, 63.4° inclination, and 270° argument of perigee. CRRESELE consists of six A_p-dependent models of the outer zone electrons, plus an Average model and a Worst-case model. The models are valid for the solar maximum period of the solar cycle. Here, we compare only the Average and Worst-case models with AE-8 MAX.

Fig. 7 shows a comparison of the electron flux predicted by the CRRESELE Average model to that predicted by AE-8. In Fig. 8, the CRRESELE Worst-case model and FLUMIC, also a worst-case model, are compared to AE-8. CRRESELE Average model differs only by a factor of 1.5 from AE-8 for energies below 1 MeV; however, CRRESELE Worst-case model suggests flux in this energy range can be more than a factor of ten greater than that predicted by AE-8 for this orbit. Conversely, FLUMIC suggests AE-8 may be a factor of three or more too high at energies below 1 MeV.

For electron energies above 1 MeV at this orbit, CRRESELE Average model under-predicts AE-8 by as much as a factor of 16 (at 4 MeV). The CRRESELE Worst-case model over-predicts AE-8 by a factor of two before significantly diverging from AE-8 above 4 MeV (Fig. 8). FLUMIC hovers below AE-8 by about a factor of 2.5 before gradually converging at energies above 5 MeV.

The integral flux values predicted by AE-8 MAX for electron energy minima of 0.5 MeV, 1 MeV, 2 MeV, and 4 MeV are shown in Table 5, along with the factor differences between the newer model predictions and AE-8.

2) Geostationary Orbit

Average integral electron flux was determined from AE-8 MAX, POLE, CRRESELE Average and Worst-case models, and FLUMIC, for a geostationary orbit of 35,790 km altitude at 82°W longitude. POLE consists of three models: Best-case, Average, and Worst-case; we show results from only the

Average and Worst-case models.

The CRRESELE Average and POLE Average models are compared with AE-8 in Fig. 9 for solar maximum. Fig. 10 shows the CRRESELE Worst-case, POLE Worst-case, and FLUMIC flux predictions for solar maximum compared to AE-8. At the 40 keV terminus of AE-8, POLE Average model predicts a factor of 1.5 greater flux, with POLE Worst-case model approaching a factor of 2.5 greater. For energies between 70 keV and 2.5 MeV, POLE Average model predicts less average flux by as much as a factor of five (at 1 MeV). POLE Worst-case model reduces this factor to between two and three, over a smaller energy range. See Table 6 for factor differences with AE-8 at specific energy levels.

The CRRESELE models tell a different story. The Average model under-predicts AE-8 by a factor of ten initially, then drops to as much as 690 times below AE-8 at 3.5 MeV. On the other hand, the Worst-case CRRESELE model varies within a factor of three above or below AE-8 for most of the shared energy range for this orbit.

FLUMIC, a worst-case model, under-predicts AE-8 by as much as a factor of 28 at 0.2 MeV, before coming within a factor of 3 below AE-8 at about 1.5 MeV. Both CRRESELE Worst-case model and FLUMIC predict greater average flux at 5 MeV and higher at this orbit. Once again, a table of selected energy points is provided that shows the AE-8 MAX predicted average flux along with the factors by which the newer models differ (Table 6).

At geostationary orbits, AE-8 MIN and AE-8 MAX do not differ. The proposed standard model for this region, POLE, demonstrates higher average electron flux during solar minimum than during solar maximum [23]. This result is also seen with the FLUMIC model [22]. Fig. 11 shows the POLE Average model predictions for solar minimum and solar maximum as compared to AE-8 (MAX) for the GEO orbit examined here. Based on the POLE model results, the difference between solar cycle periods becomes more pronounced with increasing electron energy.

IV. SUMMARY

Since the release of AP-8 and AE-8, initiatives by both NASA's Living With a Star Targeted Research and Technology Program and its Space Environments and Effects Program, ESA's Technology Research Programme, and the U.S. Air Force Space Radiation Effects Program have stimulated further model development. We have examined some of these newer models with respect to AP-8 and AE-8, for specific orbits. This paper is intended to assist spacecraft designers; for this end, we have chosen commonly used orbits that lie within the bounds of each model's validity. Providing model comparisons comes with the risk that the results will be extracted from their context and used for orbits other than those to which they apply; however, as we anticipate the standardization of new models, it is important to understand how these models differ from the tools currently available.

All of the proton models evaluated suggest that during solar minimum periods at an ISS-like orbit, AP-8 under-predicts flux for protons greater than 10 MeV. For protons having less than 10 MeV of energy, TPM-1 indicates that AP-8 may over-predict the flux at solar minimum. This pattern is seen for the polar LEO used in this paper, though with 8 MeV being the crossing point.

At the MEO examined in this paper, both TPM-1 and CRRESPRO predict less flux than AP-8 during quiet geomagnetic conditions at solar maximum, for the entire shared energy range. For active geomagnetic conditions at solar maximum, CRRESPRO tends towards agreement with AP-8, though TPM-1 continues to suggest lower flux levels.

The electron flux graphs for MEO show a murkier picture. The CRRESELE Average model indicates a softer spectrum for solar maximum at the sampled orbit. The worst-case model, FLUMIC, suggests that AE-8 MAX over-predicts electron flux for energies less than 5 MeV. Conversely, CRRESELE Worst-case model suggests that AE-8 greatly under-predicts the worst-case electron flux below 1 MeV and above 5 MeV during solar maximum.

At 82°W longitude GEO, AE-8 may over-predict the flux of electrons between 100 keV to 2.5 MeV during average solar maximum conditions. The POLE models suggest that AE-8 may under-predict electron flux at energies below 70 keV. The worst-case models do not form a consensus as to whether AE-8 under- or over-predicts electron flux during more extreme conditions of solar maximum. Finally, we note that, as expected from the literature [22]-[23], the post-AE-8 models POLE and FLUMIC demonstrate a solar cycle variation in flux for this GEO orbit, with higher flux occurring at solar minimum.

V. CONCLUSION

Accurate space radiation environment models are crucial to planning and operating missions. Models with smaller margins of error in radiation environment estimates will prevent costly over-design and will aid in the decision to use or forego a particular capability. This paper provides an overview of advances made in these efforts, including model comparisons for commonly used orbits.

At this time, we cannot make an endorsement of any particular model. The international COSPAR/PRBEM will play a central role in decisions to standardize new models. Until new standards have been established, the information provided in this paper can be used to assist spacecraft designers in deciding appropriate design margins of error.

REFERENCES

[1] D. M. Sawyer and J. I. Vette, "AP-8 trapped proton environment for solar maximum and solar minimum," NASA TM-X-72605, 1976.

[2] J. I. Vette, "The AE-8 trapped electron model environment," NSSDC/WDC-A-R&S 91-24, 1991.

[3] J. I. Vette, K. W. Chan, and M. J. Teague, "Problems in modeling the Earth's trapped radiation environment," NASA TM-80447, 1978.

[4] B. Abel, M. Thorne, and A. L. Vampola, "Solar cyclic behavior of trapped energetic electrons in Earth's inner radiation belt," *J. Geophys. Res.*, vol. 99, no. A10, pp. 19,427-19,431, 1994.

[5] D. Heynderickx, "Comparison between methods to compensate for the secular motion of the south Atlantic anomaly," *Rad. Meas.*, vol. 26, no. 3, pp. 369-373, 1996.

[6] C. S. Dyer, "Space radiation environment dosimetry," *IEEE NSREC Short Course Notes*, Ch. 2, Newport Beach, CA, USA, 1998.

[7] E. J. Daly and H. D. R. Evans, "Problems in radiation environment models at low altitudes," *Rad. Meas.*, vol. 26, no. 3, pp. 363-368, 1996.

[8] J. B. Blake, W. A. Kolasinski, R. W. Fillius, and E. G. Mullen, "Injection of electrons and protons with energies of tens of MeV into L<3 on Mar. 24, 1991," *Geophys. Res. Lett.*, vol. 19, p. 821, 1992.

[9] J. Mazur, "The radiation environment outside and inside a spacecraft," *IEEE NSREC Short Course Notes*, Ch. 2, Phoenix, AZ, USA, 2002.

[10] T. W. Armstrong and B. L. Colburn, "Evaluation of trapped radiation model uncertainties for spacecraft design," NASA/CR-2000-210072, 2000.

[11] M. S. Gussenhoven, E. G. Mullen, and D. H. Brautigam, "Near-earth radiation model deficiencies as seen on CRRES," *Adv. Space Res.*, vol. 14, no. 10, pp. 927-941, 1994.

[12] E. J. Daly, J. Lemaire, D. Heynderickx, and D. J. Rodgers, "Problems with models of the radiation belts," *IEEE Trans. Nucl. Sci.*, vol. 43, no. 2, pp. 403-415, 1996.

[13] D. Heynderickx, "Review on modeling of the radiation belts," *Int. J. Mod. Phys.A*, vol. 17, nos. 12&13, pp. 1675-1684, 2002.

[14] T. W. Armstrong and B. L. Colburn, "Trapped radiation model uncertainties: Model-data and model-model comparisons," NASA/CR-2000-210071, 2000.

[15] J. Barth, "Modeling space radiation environments," *IEEE NSREC Short Course Notes*, Ch. 1, Snowmass, CO, USA, 1997.

[16] J. I. Vette, "The NASA/National Space Science Data Center Trapped Radiation Environment Model Program (1964-1991)," NSSDC/WDC-A-R&S 91-29, 1991.

[17] D. Heynderickx, M. Kruglanski, V. Pierrard, J. Lemaire, M. D. Looper, and J. B. Blake, "A low altitude trapped proton model for solar minimum conditions based on SAMPEX/PET data," *IEEE Trans. Nucl. Sci.*, vol. 46, no. 6, 1999.

[18] S. L. Huston, "Space Environments and Effects: Trapped Proton Model," NASA/CR-2002-211784, 2002.

[19] D. M. Boscher, S. A. Bourdarie, R. H. W. Friedel, and R. D. Belian, "Model for the geostationary electron environment: POLE," *IEEE Trans. Nucl. Sci.*, vol. 50, no. 6, pp. 2278-2283, 2003.

[20] S. L. Huston and K. A. Pfitzer, "Space Environment Effects: Low-Altitude Trapped Radiation Model," NASA/CR-1998-208593, 1998.

[21] M. S. Gussenhoven, E. G. Mullen, M. D. Violet, C. Hein, J. Bass, and D. Madden, "CRRES high energy proton flux maps," *IEEE Trans. Nucl. Sci.*, vol. 40, no. 6, pp. 1450-1457, 1993.

[22] G. L. Wrenn, D. J. Rodgers, and P. Buehler, "Modeling the outer belt enhancements of penetrating electrons," *J. Spacecraft Rockets*, vol. 37, no. 3, pp. 408-415, 2000.

[23] D. H. Brautigam, M. S. Gussenhoven, E. G. Mullen, "Quasi-static model of outer zone electrons," *IEEE Trans. Nucl. Sci.*, vol. 39, no. 6, 1992.

[24] A. L. Vampola, "Low energy inner zone protons—revisited," in *AIP Conf. Proc. 383*, New York, 1996, pp. 81-86.

TABLE I. RADIATION BELT MODELS BY REGION OF COVERAGE

ORBIT	MODEL	DEVELOPER	DATA SOURCE, EPOCH	PARTICLE, ENERGY RANGE	FEATURES	AVAILABILITY
LEO: L=1.1-2.0	PSB97 (proposed standard)	BIRA/ Aerospace Corp., 1997 [17]	SAMPEX-PET 1995	Directional, differential/ integral protons 18.5 – 500 MeV	Valid for solar minimum Internal field model	SPENVIS
LEO: 250-850 km	LATRM (formerly NOAAPRO)	The Boeing Co., 1998 [18]	TIROS/NOAA 11/78-10/95 (6 satellites)	Omnidirectional, integral protons >16, >30, >80 MeV	True solar-cycle variation using $F_{10.7}$ proxy for driver Internal field model Secular var. of B_{Earth}	NASA/MSFC-SEE Program
LEO, MEO: 300 km-<GEO	TPM-1 (proposed standard)	S.L. Huston The Boeing Co., 2002 [19]	TIROS/NOAA 11/78-10/95 CRRES-PROTEL 7/90-10/91	Omnidirectional, differential protons 1.5 – 81.3 MeV	Low alt. solar-cycle variation using $F_{10.7}$ proxy for driver Internal field model Secular var. of B_{Earth} 1 month time resolution Quiet/Active (K_p) models	NASA/MSFC-SEE Program
MEO: L=1.4-5.5	CRRESPRO	AFRL, 1993 [20]	CRRES-PROTEL 7/90-10/91	Omnidirectional, differential/integral protons 1 – 100 MeV	Valid for solar maximum Quiet/Active (K_p) models Internal & external field models	AFRL/VSBXR, SPENVIS
MEO, GEO: L=2.4-6.8	CRRESELE	AFRL, 1992 [21]	CRRES-HEEF 7/90-10/91	Omnidirectional, differential/integral electrons 0.5 – 6.6 MeV	Driven by Ap_{15} Internal & external field models, plus 6 Ap_{15}-dependent models, plus average & worst-case models Valid for solar maximum Outer electron belt only	AFRL/VSBXR, SPENVIS
MEO, GEO: L=3-8	FLUMIC	DERA, 1999 [22]	GOES-7 1987-1998 LANL GEO ESP 9/89-10/98 STRV-1b-REM 8/94-5/98	Directional, integral electrons > 0.2 to > 5.9 MeV (20 increments)	Worst-case 1-day fluence Code adjustable to reflect worst cases due to SPEs/CMEs Solar-cycle variation	SPENVIS, QinetiQ
GEO	POLE (proposed standard)	LANL/ONERA, 2003 [23]	LANL GEO CPA/SOPA 1976-2001 (13 satellites)	Omnidirectional, differential/integral electrons 0.03 – 2.5 MeV	Internal & external field models Created for DICTAT, an internal charging model Mean, worst- and best-case models Solar-cycle variation (data from 2.5 cycles) 1 year time resolution	ONERA/DESP, TRAD: OMERE

Selected abbreviations: Ap_{15}, a 15-day average of a geomagnetic activity index (Ap is based upon Kp); B_{Earth}, Earth's magnetic field; BIRA, Belgian Institute for Space Aeronomy; CME, coronal mass ejection; DESP, Space Environment Department; Kp, index of worldwide average level of geomagnetic activity; MEO, medium Earth orbit; MSFC, Marshall Space Flight Center; SPE, solar proton event; VSBXR, Space Vehicles Directorate Battlespace Environment Division
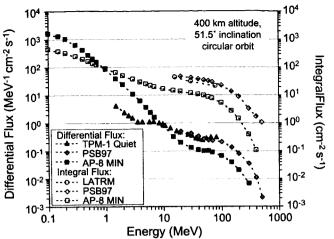
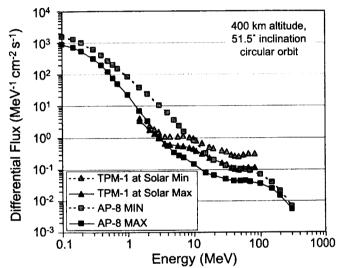Fig. 1. Average proton flux at solar minimum for a circular orbit at 400 km altitude and 51.6° inclination.

Fig. 2. Proposed standard TPM-1 model at solar minimum versus solar maximum for a circular orbit at 400 km altitude and 51.6° inclination.
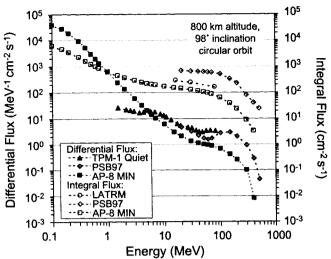

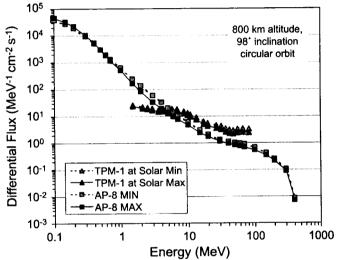Fig. 3. Average proton flux at solar minimum for a circular orbit at 800 km altitude and 98° inclination.

Fig. 4. Proposed standard TPM-1 model at solar minimum versus solar maximum for a circular orbit at 800 km altitude and 98° inclination.

TABLE II. AP-8 PREDICTED AVERAGE PROTON FLUX AND RATIOS OF NEW MODEL FLUX TO AP-8 FLUX, FOR A CIRCULAR ORBIT AT 400 KM ALTITUDE AND 51.6° INCLINATION.

	Integral flux comparison			Differential flux comparison				
Energy (MeV)	AP-8 MIN (cm⁻² s⁻¹)	PSB97 solar min (ratio)	LATRM solar min (ratio)	AP-8 MIN (MeV⁻¹ cm⁻² s⁻¹)	PSB97 solar min (ratio)	TPM-1 solar min (ratio)	AP-8 MAX (MeV⁻¹ cm⁻² s⁻¹)	TPM-1 solar max (ratio)
1.5	442			235		0.11	159	0.15
20	143	5.0	1.9	2.1	2.3	2.5	1.7	2.5
60	96	6.4	2.0	0.94	1.7	3.7	0.74	3.4
100	65	8.2		0.67	4.2		0.54	

TABLE III. AP-8 PREDICTED AVERAGE PROTON FLUX AND RATIOS OF NEW MODEL FLUX TO AP-8 FLUX, FOR A CIRCULAR ORBIT AT 800 KM ALTITUDE AND 98° INCLINATION.

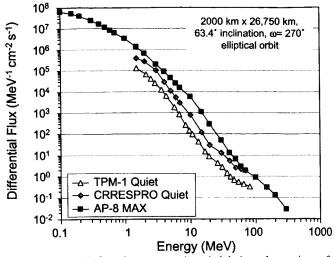|	Integral flux comparison			Differential flux comparison				
Energy (MeV)	AP-8 MIN (cm⁻² s⁻¹)	PSB97 solar min (ratio)	LATRM solar min (ratio)	AP-8 MIN (MeV⁻¹ cm⁻² s⁻¹)	PSB97 solar min (ratio)	TPM-1 solar min (ratio)	AP-8 MAX (MeV⁻¹ cm⁻² s⁻¹)	TPM-1 solar max (ratio)
1.5	64			38		0.11	6.8	0.51
20	13	3.5	2.9	0.20	2.5	2.4	6.4x10⁻²	3.1
60	8.6	3.7	2.7	0.10	2.5	3.1	4.3x10⁻²	2.8
100	5.3	4.2		6.8x10⁻²	3.2		3.5x10⁻²	

Fig. 5. Proton models for quiet geomagnetic period during solar maximum for a 2000 km x 26,750 km, 63.4° inclination, ω=270°, elliptical orbit.

Fig. 7. CRRESELE Average model versus AE-8 MAX at solar maximum for an 8000 km x 26,750 km, 63.4° inclination, ω=270°, elliptical orbit.
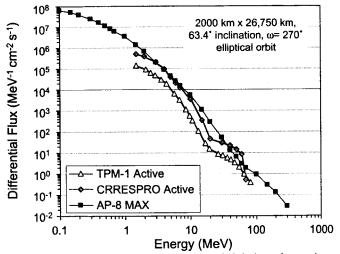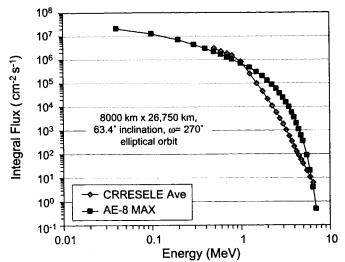

Fig. 6. Proton models for active geomagnetic period during solar maximum for a 2000 km x 26,750 km, 63.4° inclination, ω=270°, elliptical orbit.
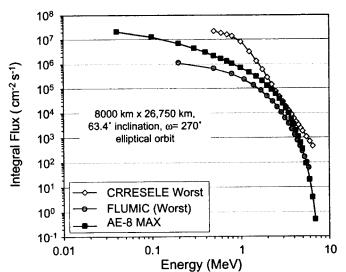

Fig. 8. Worst-case electron models versus AE-8 MAX at solar maximum for an 8000 km x 26,750 km, 63.4° inclination, ω=270°, elliptical orbit.

TABLE IV. AP-8 PREDICTED AVERAGE PROTON FLUX AND RATIOS OF NEW MODEL FLUX TO AP-8 FLUX, FOR A 2000 KM X 26,750 KM, 63.4° INCLINATION, ω=270°, ELLIPTICAL ORBIT.

Energy (MeV)	AP-8 MAX (MeV^{-1} cm^{-2} s^{-1})	TPM-1 Quiet (ratio)	CRRESPRO Quiet (ratio)	TPM-1 Active (ratio)	CRRESPRO Active (ratio)
1.5	1.4x10^6	0.098	0.29	0.11	0.37
10	5.5x10^3	0.024	0.14	0.089	0.62
20	283	0.030	0.11	0.053	0.17
60	2.9	0.17	0.78	0.51	3.0

TABLE V. AE-8 PREDICTED AVERAGE ELECTRON FLUX AND RATIOS OF NEW MODEL FLUX TO AE-8, FOR A 2000 KM X 26,750 KM, 63.4° INCLINATION, ω=270°, ELLIPTICAL ORBIT.

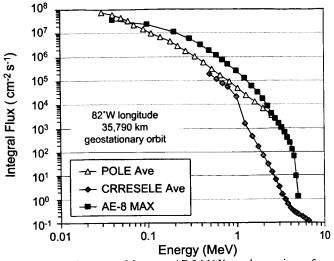| Energy (MeV)	AE-8 MAX (cm^{-2} s^{-1})	CRRESELE Average (ratio)	CRRESELE Worst-case (ratio)	FLUMIC (ratio)
0.5	2.1x10^6	1.5	10	0.31
1	7.0x10^5	1.2	12	0.40
2	1.3x10^5	0.17	2.2	0.37
4	3.4x10^3	0.061	1.8	0.44

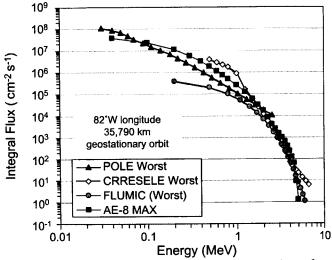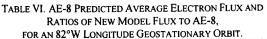Fig. 9. Average electron models versus AE-8 MAX at solar maximum for an 82°W longitude geostationary orbit.

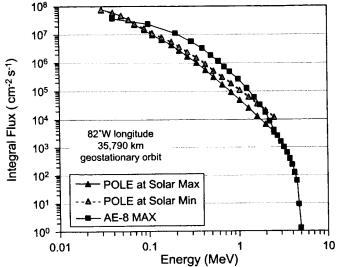Fig. 11. Proposed standard POLE model predictions for solar maximum and solar minimum at 82°W longitude geostationary orbit.

Fig. 10. Worst-case models versus AE-8 MAX at solar maximum for an 82°W longitude geostationary orbit.

TABLE VI. AE-8 PREDICTED AVERAGE ELECTRON FLUX AND
RATIOS OF NEW MODEL FLUX TO AE-8,
FOR AN 82°W LONGITUDE GEOSTATIONARY ORBIT.

Energy (MeV)	AE-8 MAX (cm^{-2} s^{-1})	POLE Average (ratio)	POLE Worst-case (ratio)	CRRESELE Average (ratio)	CRRESELE Worst-case (ratio)	FLUMIC (ratio)
0.05	3.3×10^7	1.4	2.0			
0.5	1.8×10^6	0.21	0.37	0.11	2.1	0.11
1	2.6×10^5	0.20	0.42	0.084	3.3	0.23
2	1.7×10^4	0.40	1.1	4.1×10^{-3}	0.68	0.39
4	230			1.7×10^{-3}	0.31	0.31